ACS APPLIED MATERIALS & INTERFACES

Letter

www.acsami.org

Fabrication of Electrically Conductive Metal Patterns at the Surface of Polymer Films by Microplasma-Based Direct Writing

Souvik Ghosh,[†] Rui Yang,[‡] Michelle Kaumeyer,[‡] Christian A. Zorman,[‡] Stuart J. Rowan,[§]
Philip X.-L. Feng,[‡] and R. Mohan Sankaran*,[†]

[†]Department of Chemical Engineering, [‡]Department of Electrical Engineering and Computer Science, and [§]Department of Macromolecular Sciences and Engineering, Case Western Reserve University, Cleveland, Ohio, United States

Supporting Information

ABSTRACT: We describe a direct-write process for producing electrically conductive metal patterns at the surface of polymers. Thin films of poly(acrylic acid) (PAA) loaded with Ag ions are reduced by a scanning, atmospheric-pressure microplasma to form crystalline Ag features with a line width of 300 μm. Materials analysis reveals that the metallization occurs in a thin layer of ∼5 μm near the film surface, suggesting that the Ag ions diffuse to the surface. Sheet resistances of 1−10 Ω/sq are obtained independent of film thickness and Ag volume concentration, which is desirable for producing surface conductivity on polymers while minimizing metal loading.

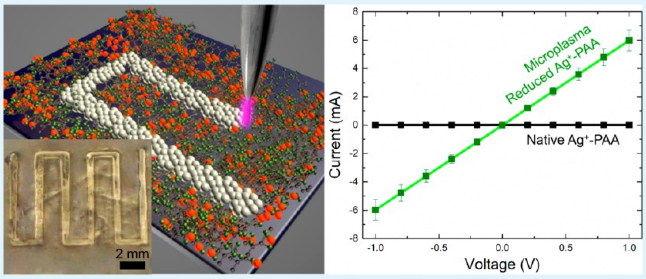

KEYWORDS: *microplasma, direct write, electrodiffusion, printed electronics, flexible electronics, sheet resistance*

INTRODUCTION

Patterning metal as a contact or interconnect is a critical processing step for device fabrication in a wide range of applications. Traditionally, physical vapor deposition (PVD) is combined with lithography to first deposit a metal film such as Ag, then remove the undesired areas to produce a pattern. Although this subtractive approach has high fidelity and results in an electrically conductive metal layer without any thermal annealing, the low throughput, materials wastage, and need for vacuum lead to high operating costs and limited scalability.[1] Recently, the emergence of flexible electronic devices has stimulated the desire for alternative, additive approaches for fabricating patterned metal features. Some examples of techniques that have been developed include inkjet printing,[2,3] screen printing,[4,5] aerosol printing,[6,7] and nanoimprint lithography.[8,9] A common feature of these processes is the inks, which typically comprise organic-ligand stabilized dispersions of metal nanoparticles[2] or metal−organic compounds.[3,10,11] An advantage of ink-based printing methods is that the processes are carried out at ambient conditions and therefore can be easily integrated with roll-to-roll systems for large-scale manufacturing.[1,12] However, the inks themselves are usually expensive due to the number of processing steps associated with synthesis, dispersion, purification, and concentration. In addition, the as-deposited films often exhibit poor conductivity requiring a postdeposition annealing step, which may not be compatible with some polymer substrates.[13] Highly conductive films have been produced at room temperature by electroless deposition where the metal is chemically reduced onto a polymeric substrate from solution.[14−16] Electroless processes require an initial metal layer that is often prepared by inkjet printing to serve as activation sites and obtain patterned deposits.[17,18] Alternatively, patterns of metallic features have been directly written by exposing polymer films containing a metal precursor to a laser[19,20] or electron beam.[21] Unfortunately, these processes remain complex and in many cases require annealing to produce reasonable conductivity.

Here, we present a direct-write process at ambient conditions to produce electrically conductive metal patterns at the surface of polymer films. The process bears similarities with electron-beam assisted nanofabrication, but does not require vacuum, postannealing, or complex equipment. Polymer films are first prepared with a metal phase and then exposed to a scanning, nonthermal, atmospheric-pressure microplasma. Localized reactions between the electrons in the microplasma and metal ions in the film result in reduction, nanoparticle nucleation and growth, and aggregation of the nanoparticles into a percolating network of electrically conductive metal particles. A particularly unique aspect of the process is that the metallization occurs near the film surface which we propose occurs via electrodiffusion of the metal ions in the electric field created by the microplasma. Thus, highly conductive films with a sheet resistance as low as 1 Ω/sq are produced at relatively low metal loading in the polymer film.

EXPERIMENTAL PROCEDURE

Thin films of poly(acrylic acid) (PAA) loaded with silver cations (Ag^+) were prepared by solution methods. PAA (Acros

Received: December 27, 2013
Accepted: February 20, 2014
Published: February 20, 2014

dx.doi.org/10.1021/am406005a | ACS Appl. Mater. Interfaces 2014, 6, 3099−3104

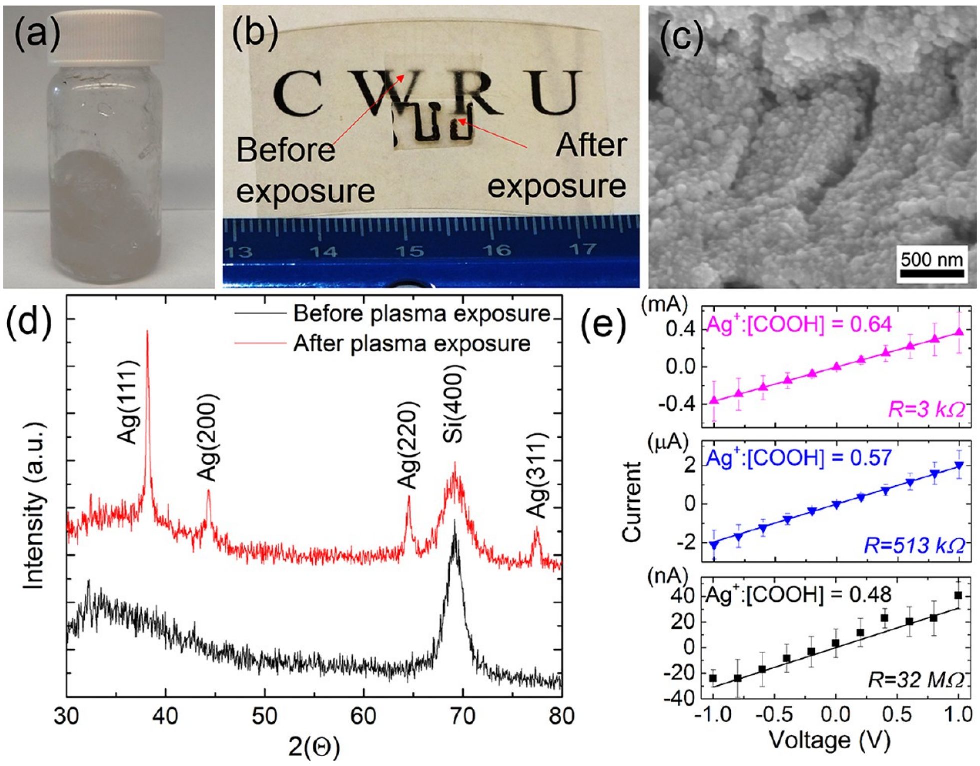

Figure 1. (a) Optical image of Ag/PAA after formation of gel precipitate (Ag^+:[COOH] = 0.64:1). (b) Optical images of Ag/PAA films on a PET sheet with the letters "CWRU" behind on paper, before and after microplasma exposure. The films were transferred by peeling off the Si substrate. (c) SEM image of microstructure of Ag/PAA film (Ag^+:[COOH] = 0.64:1) showing network of Ag particles after microplasma reduction. (d) XRD of Ag/PAA films (Ag^+:[COOH] = 0.64:1) showing the formation of crystalline Ag after microplasma exposure. (e) Current−voltage characteristics of microplasma-reduced lines, each 300 μm × 5 mm, on 8 μm thick films as a function of the Ag^+:[COOH] ratio.

Organic, M_w = 1 260 000) was dissolved in 100 mL of 1:3 v/v deionized water:ethanol at 0.255% w/v. Silver nitrate ($AgNO_3$, >99.9% purity, Alfa Aesar) dissolved in 20 mL of the same solvent was added to the solution and stirred vigorously for 10 min. An additional 150 mL of ethanol was then added to this mixture and left to stir for another 15 min. The resultant milky white solution was centrifuged and a white precipitate containing the PAA and Ag^+ was collected after decanting the clear supernatant. The precipitate was homogenized in 6:1 v/v water:ethylene glycol at 10−20% w/w (Cole Parmer, LabGen 7). After homogenizing, the sample was kept in vacuum (approximately −20 psi) for a minute to remove air bubbles. The resulting fluid was cast with a doctor's blade on n-type silicon (Si) (100) wafers, dried overnight, and finally vacuum-dried for 2 h before microplasma exposure. The Ag concentration in the deposited film was calculated as the molar ratio of Ag^+ to repeat units of PAA, i.e., ($CH(COOH)CH_2$), represented as [COOH], in the solution. For example, a film containing Ag^+:[COOH] = 1:1 indicates that 169.87 g of $AgNO_3$ was mixed with 72 g of PAA in solution.

Patterns of reduced Ag were fabricated by exposing the Ag/PAA film to a scanning, nonthermal, atmospheric-pressure microplasma. Details of the microplasma setup are described elsewhere.[22,23] Here, we formed a microplasma in a flow of argon (Ar) gas at 700 V and 1 mA with a cathode to anode gap of 500 μm. The microplasma was scanned across the film by moving the substrate in two dimensions with a pair of computer-controlled stepper motors. A minimum average line width of 300 μm was obtained at a scan rate of 250 μm/s (see the Supporting Information).

After microplasma exposure, the processed film was peeled off from the Si substrate and placed on an insulating substrate such as glass or polyethylene terephthalate (PET). Conductive Ag paste was used to deposit contact pads on the microplasma-reduced features for current−voltage (I−V) measurements. Electrical characterization was performed inside a Faraday chamber with a two-point probe setup using a Keithley 4200 SCS source which can precisely measure resistances ranging from 1×10^{-6} to 1×10^{12} Ω.

Scanning electron microscopy (SEM), focused ion beam (FIB) etching, and energy dispersive spectroscopy (EDX) were performed with a FEI Nova Nanolab 200 field-emission gun SEM. The polymer samples were sputter coated with 5 nm Pd prior to SEM.

■ RESULTS AND DISCUSSION

A key part of this study was the selection of the metal (and corresponding metal precursor) and polymer to be exposed to the scanning microplasma process to obtain electrically conductive patterns. We focused on water-soluble metal salts and polymers that are widely used, safe, low cost, and easy to solution process. We chose Ag as the metal because it is an excellent conductor, easy to reduce [standard reduction potential = 0.799 V vs standard hydrogen electrode (SHE)], is significantly less expensive than other metals such as Au, and has a readily available water-soluble salt, $AgNO_3$. Polyacrylic acid (PAA) was selected as the polymer because it is also water-soluble, and has been previously reported to electrostatically bind with different metal cations, including Ag^+, through its carboxylic acid (−COOH) side chains.[24−26] After loading, the solubility in polar solvents is reduced, facilitating recovery of the metal ion-polymer mixture. Figure 1a shows an image of the Ag/PAA gel precipitate after separation from the supernatant. Casting using a doctor's blade produces a semitransparent film containing only the polymer and Ag^+ (Figure 1b). Exposing to the microplasma results in a clear color change attributed to the formation of metallic Ag at the surface of the film (Figure 1b). A representative scanning electron microscope (SEM) image of a patterned line on a film containing Ag^+:[COOH] = 0.64 reveals the presence of particles within the feature, presumably Ag, forming a relatively uniform and continuous network (Figure 1c). X-ray diffraction (XRD) confirmed that the patterned line consisted of crystalline Ag [Figure 1(d)]. We similarly prepared 5 μm thick Ag/PAA films containing different ratios of Ag^+:[COOH] ranging from 0.32:1 to 0.64:1. Figure 1e shows I−*V* characteristics of the 5 mm long patterned lines produced upon exposure to plasma. With increasing concentration of Ag^+ in the polymer, the resistances determined from the average slope were found to decrease from 32 MΩ to 3 kΩ, consistent with higher Ag^+:[COOH] ratios leading to more conductive networks.

To further examine the microplasma-reduced lines and understand the nature of particle formation and conductivity, we carried out additional SEM and energy-dispersive spectroscopic (EDX) analyses. Images a and b in Figure 2 show SEM images and corresponding EDX maps of lines patterned in a relatively low Ag concentration (Ag^+:[COOH] = 0.32:1) film by the microplasma. The EDX maps are false colored with the intensity corresponding to the Ag content in the film. The high intensity of Ag confirms that Ag ions are reduced, leading to particle nucleation and growth in the patterned region [Figure 2(b)]. In order to analyze the concentration of Ag within the film, a 5 μm deep trench was created across the patterned line by focused ion beam (FIB). The EDX map suggests that the Ag concentration is higher near the surface [Figure 2(b)]. To more carefully characterize the concentration depth profile, films were cut and SEM images and corresponding EDX false color intensity maps were obtained (Figure 2c−h). The cross-sectional analysis shows high surface concentration of Ag, confirming that the reduction and formation of Ag particles is localized near the surface (Figure 2c, d). This is further supported by images near the edge of a patterned line that show the nonuniform Ag concentration only occurs in the exposed part of the film (Figure 2e, f). Images of the unexposed region of the same film show that without plasma exposure, the Ag ion concentration is homogeneous throughout the film depth (Figure 2g, h). The cross-sectional images were semiquantitatively analyzed by plotting the intensity of the EDX line scan as a function of film depth (Figure 3). SEM images of the EDX scan areas are also shown in Figure 3 for reference. We find that in the native film, the Ag and C concentrations are constant throughout the film at an atomic percent of 25 at % Ag and 50 at % C. The Ag concentration rapidly increases after microplasma exposure at the film surface to ~75 at %, and, simultaneously, the C concentration decreases to ~25 at %. Moving down from the film surface, the Ag concentration rapidly decreases from 75 at % at ~5 μm and reaches its original value of 25 at % at a depth of ~10 μm. Near the base of the film, the C concentration increases to ~75 at % and the Ag concentration is depleted to ~10 at %.

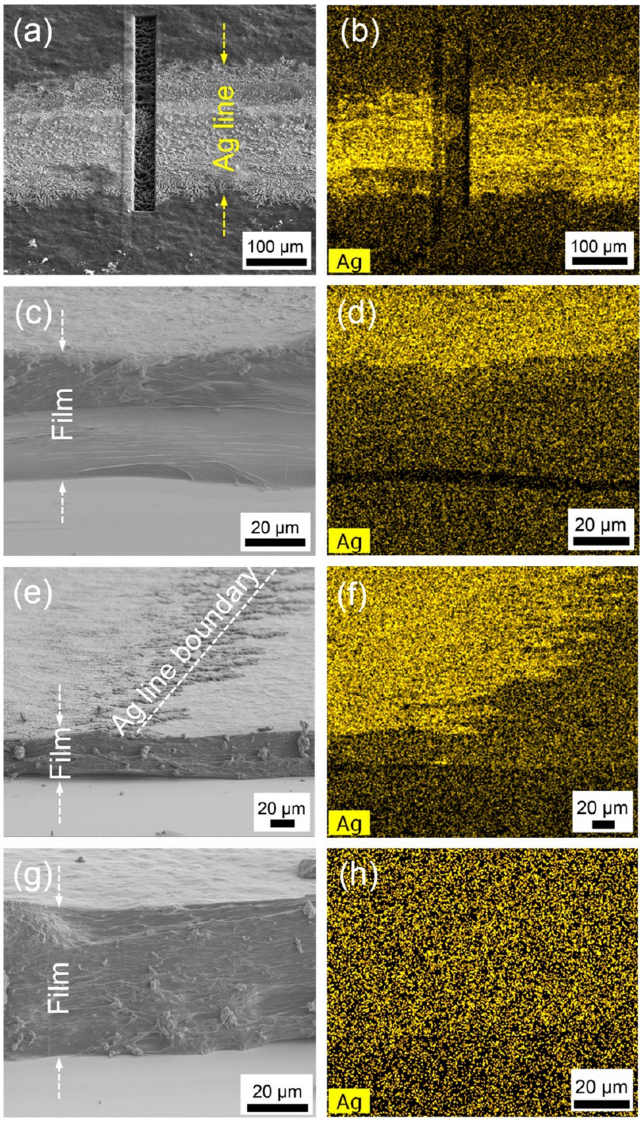

Figure 2. (a) The center of the Ag line was etched by FIB. The center of the line was etched by FIB. (b) EDX false color map of Ag in a. (c) Cross-sectional SEM image of microplasma-reduced region. (d) EDX false color map of Ag in c showing higher concentration of Ag at the surface. (e) Cross-sectional SEM image at the boundary of a microplasma-reduced line. (f) EDX false color map of Ag in (e) showing higher surface concentration of Ag only in the microplasma exposed region. (g) Cross-sectional SEM image of an unexposed region of the same sample analyzed in c−f. (h) EDX false color map of Ag in g showing uniform distribution of Ag.

The enrichment of Ag at the surface and simultaneous depletion of Ag at the base of the film after microplasma exposure suggest that surface reduction alone cannot explain the formation of an Ag-rich surface layer. We propose that Ag ions within the bulk of the film diffuse to the surface during microplasma exposure to supply metal precursor for continued growth. The DC microplasma process produces an electric field within the film oriented with a negative pole at the surface and a positive pole at the base. This electric field may drive diffusion of the positively charged Ag^+ to the film surface, termed electrodiffusion.[27] The coordination of Ag^+ to PAA is reversible[25] and the electric field should present a strong enough force to pull the Ag^+ ions to the film surface where they can undergo reduction by electrons from the microplasma. It is possible that the polymer may undergo some morphological changes during this process; however it still acts as a supporting

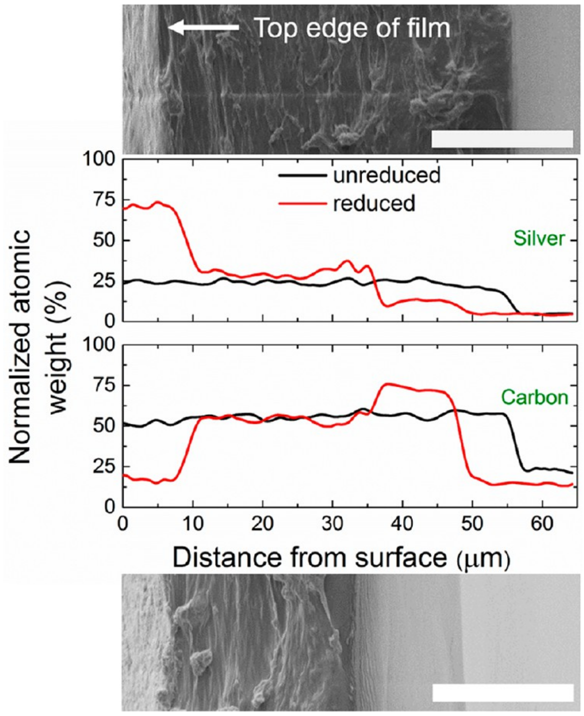

Figure 3. Cross-sectional SEM images of Ag/PAA films before (top) and after (bottom) microplasma reduction and corresponding normalized atomic weight of Ag and C through the film depth, as obtained by EDX line scans. Scale bar is 20 μm.

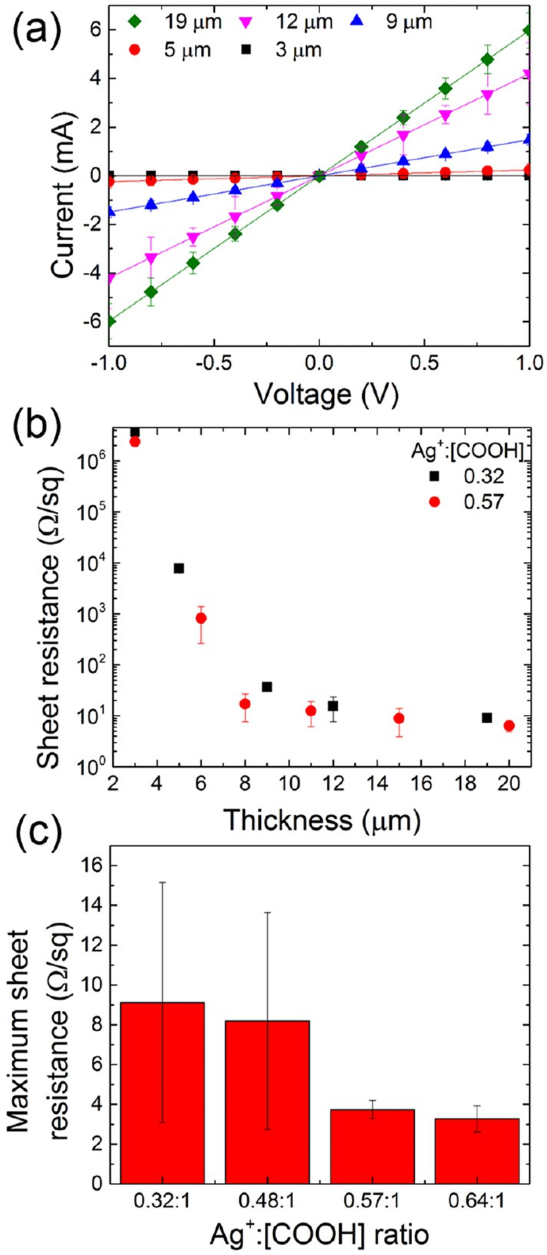

Figure 4. (a) Current−voltage characteristics of 5000 × 300 μm^2 microplasma-reduced lines in Ag^+:[COOH] = 0.32:1 films of varying thickness. The data were fitted by linear regression with a y-intercept of 0 to yield ohmic resistances of 35 MΩ, 4 kΩ, 671 Ω, 238 Ω, and 167 Ω for original film thicknesses of 3, 5, 9, 12, and 19 μm respectively. (b) Average sheet resistance as a function of original film thickness at two concentrations of Ag^+:[COOH]. (c) Maximum average sheet resistance for films of different Ag^+:[COOH] concentrations. All films had original thicknesses >20 μm.

backbone to the Ag layer on the surface. To validate this qualitative picture, we processed films of varying thickness with a low Ag content (Ag^+:[COOH] = 0.32:1). If electrodiffusion of Ag ions occurs during microplasma exposure, thicker films should provide a larger reservoir for particle growth, and thus form Ag lines with lower resistance. Figure 4(a) shows that by increasing the thickness from 3 to 20 μm, the resistance of a constant line shape of 300 μm x 5 mm decreases from approximately 30 MΩ to 200 Ω, supporting the electrodiffusion model. Consistent with this picture, the resistance on the back of the films remains high (see the Supporting Information). We also carried out several control experiments and found that neither UV light from the microplasma nor other UV sources could produce the same reduced metallic films (see the Supporting Information). This further underscores the importance of electrodiffusion which we believe is critical to the precipitation of a metallic, conductive Ag layer in our films.

The figure of merit for electrical conductivity is bulk resistivity. Bulk resistivity can be calculated from the geometry of the microplasma drawn line. The thickness of our reduced lines is not the original film thickness, but some surface layer that is on the order of ∼5 μm thick, based on cross-sectional EDX analysis (see Figure 3). Assuming this thickness, we estimated a bulk conductivity of 4.5 mΩ cm for films containing a Ag^+:[COOH] ratio of 0.32. However, the concentration of Ag in this layer is not constant and decreases moving away from the surface into the bulk of the film. Because the Ag concentration is significantly higher in this near surface region than the rest of the film, we can assume that the surface layer is the primary contributor to electrical conduction and characterize the film conductivity by the sheet resistance. Figure 4b shows sheet resistances as a function of the original film thickness after microplasma exposure for two difference ratios of Ag^+:[COOH]. For thin films (<10 μm), the Ag loading in the film volume or the exposure time (scanning rate) is too low for the Ag to diffuse to the surface and react to form a percolated network. Beyond a critical thickness of approximately ∼12 μm, the sheet resistance of the microplasma-reduced lines decreases dramatically and becomes independent of the film thickness (∼10 Ω/sq), indicating that the Ag loading is high enough to diffuse within the time scale of microplasma exposure to form a percolated network. These results indicate that the sheet resistance reaches a maximum at a sufficiently large film thickness, independent of the initial Ag^+:[COOH] concentration. Thus, the sheet resistance can be optimized for any given Ag^+:[COOH] concentration. Figure 4c shows the maximum sheet resistance obtained on films with Ag^+:[COOH] ratios of 0.32:1, 0.48:1, 0.57:1 and 0.64:1, respectively, and thicknesses >20 μm. The sheet resistances are found to be between 1 and 10 Ω/sq, independent of Ag loading. These values are comparable to Ag features obtained by inkjet printing (38 Ω/sq), screen printing (∼50 mΩ/sq),[12,28] spray deposition (∼50 Ω/sq),[29] and electroless deposition (∼0.1 mΩ/sq).[30]

CONCLUSIONS

In summary, we have developed a room condition, direct-write process based on a scanning, atmospheric-pressure microplasma to produce electrically conductive lines at the surface of polymer films. Our study suggests that the metallization occurs via electrodiffusion of Ag ions to the film surface and reduction by the microplasma. The surface conductivity is maximized independent of metal loading, which may be desirable to reduce overall metal content while producing conductivity where it is desirable for many flexible conductor applications, at the surface of the film.

ASSOCIATED CONTENT

Ⓢ Supporting Information

Additional experimental details, materials characterization, electrical measurements, and control experiments with UV sources. This material is available free of charge via the Internet at http://pubs.acs.org.

AUTHOR INFORMATION

Corresponding Author

*E-mail: mohan@case.edu.

Notes

The authors declare no competing financial interest.

ACKNOWLEDGMENTS

This work was supported by the National Science Foundation (NSF) Grant SNM-1246715. The authors acknowledge Laurie Dudik (Managing Engineer, Electronics Design Center, Case Western Reserve University) for help with the homogenizer and doctor-blade casting techniques, Dr. Ina Martin (Director, Materials for Opto-electronics Research and Education Center, Case Western Reserve University) for assistance with surface profilometry, and Prof. Harihara Baskaran (Department of Chemical Engineering, Case Western Reserve University) for access to a TC5C Centrifuge.

REFERENCES

(1) Forrest, S. R. The Path to Ubiquitous and Low-Cost Organic Electronic Appliances on Plastic. *Nature* **2004**, *428*, 911−918.

(2) Russo, A.; Ahn, B. Y.; Adams, J. J.; Duoss, E. B.; Bernhard, J. T.; Lewis, J. A. Pen-on-Paper Flexible Electronics. *Adv. Mater.* **2011**, *23*, 3426−3430.

(3) Walker, S. B.; Lewis, J. A. Reactive Silver Inks for Patterning High-Conductivity Features at Mild Temperatures. *J. Am. Chem. Soc.* **2012**, *134*, 1419−1421.

(4) Faddoul, R.; Reverdy-Bruas, N.; Blayo, A. Formulation and Screen Printing of Water Based Conductive Flake Silver Pastes Onto Green Ceramic Tapes for Electronic Applications. *Mater. Sci. Eng., B* **2012**, *177*, 1053−1066.

(5) Zhang, Y.; Zhu, P.; Li, G.; Zhao, T.; Fu, X.; Sun, R.; Zhou, F.; Wong, C.-P. Facile Preparation of Monodisperse, Impurity-Free, and Antioxidation Copper Nanoparticles on a Large Scale for Application in Conductive Ink. *ACS Appl. Mater. Interfaces* **2014**, *6*, 560−567.

(6) Zhao, D.; Liu, T.; Zhang, M.; Liang, R.; Wang, B. Fabrication and Characterization of Aerosol-Jet Printed Strain Sensors for Multifunctional Composite Structures. *Smart Mater. Struct.* **2012**, *21*, 115008.

(7) Mahajan, A.; Frisbie, C. D.; Francis, L. F. Optimization of Aerosol Jet Printing for High-Resolution, High-Aspect Ratio Silver Lines. *ACS Appl. Mater. Interfaces* **2013**, *5*, 4856−4864.

(8) Ok, J. G.; Kwak, M. K.; Huard, C. M.; Youn, H. S.; Guo, L. J. Photo−Roll Lithography (PRL) for Continuous and Scalable Patterning with Application in Flexible Electronics. *Adv. Mater.* **2013**, *25*, 6554−6561.

(9) Ahn, S. H.; Guo, L. J. Large-Area Roll-to-Roll and Roll-to-Plate Nanoimprint Lithography: A Step toward High-Throughput Application of Continuous Nanoimprinting. *ACS Nano* **2009**, *3*, 2304−2310.

(10) Jahn, S. F.; Blaudeck, T.; Baumann, R. R.; Jakob, A.; Ecorchard, P.; Ruffer, T.; Lang, H.; Schmidt, P. Inkjet Printing of Conductive Silver Patterns by Using the First-Aqueous Particle-Free MOD Ink without Additional Stabilizing Ligands. *Chem. Mater.* **2010**, *22*, 3067−3071.

(11) Komoda, N.; Nogi, M.; Suganuma, K.; Otsuka, K. Highly Sensitive Antenna Using Inkjet Overprinting with Particle-Free Conductive Inks. *ACS Appl. Mater. Interfaces* **2012**, *4*, 5732−5736.

(12) Hosel, M.; Sondergaard, R. R.; Angmo, D.; Krebs, F. C. Comparison of Fast Roll-to-Roll Flexographic, Inkjet, Flatbed, and Rotary Screen Printing of Metal Back Electrodes for Polymer Solar Cells. *Adv. Eng. Mater.* **2013**, *15*, 995−1001.

(13) Perelaer, J.; Smith, P. J.; Mager, D.; Soltman, D.; Volkman, S. K.; Subramanian, V.; Korvink, J. G.; Schubert, U. S. Printed Electronics: The Challenges Involved in Printing Devices, Interconnects, and Contacts Based on Inorganic Materials. *J. Mater. Chem.* **2010**, *20*, 8446−8453.

(14) Bessueille, F.; Gout, S.; Cotte, S.; Goepfert, Y.; Leonard, D.; Romand, M. Selective Metal Pattern Fabrication Through Micro-Contact or Ink-Jet Printing and Electroless Plating onto Polymer Surfaces Chemically Modified by Plasma Treatments. *J. Adhes.* **2009**, *85*, 690−710.

(15) Wolf, S.; Feldmann, C. $Cu_2X(OH)_3$ ($X = Cl^-, NO_3^-$): Synthesis of Nanoparticles and Its Application for Room Temperature Deposition/Printing of Conductive Copper Thin-Films. *J. Mater. Chem.* **2010**, *20*, 7694−7699.

(16) Liao, Y.-C.; Kao, Z.-K. Direct Writing Patterns for Electroless Plated Copper Thin Film on Plastic Substrates. *ACS Appl. Mater. Interfaces* **2012**, *4*, 5109−5113.

(17) Cheng, K.; Yang, M.-W.; Chiu, W. W. W.; Huang, C.-Y.; Chang, J.; Ying, T.-F.; Yang, Y. Ink-Jet Printing, Self-Assembled Polyelectrolytes, and Electroless Plating: Low Cost Fabrication of Circuits on a Flexible Substrate at Room Temperature. *Macromol. Rapid Commun.* **2005**, *26*, 247−264.

(18) Garcia, A.; Polesel-Maris, J.; Viel, P.; Palacin, S.; Berthelot, T. Localized Ligand Induced Electroless Plating (LIEP) Process for the Fabrication of Copper Patterns Onto Flexible Polymer Substrates. *Adv. Funct. Mater.* **2011**, *21*, 2096−2102.

(19) Stellacci, F.; Batter, C. A. Laser and Electron-Beam Induced Growth of Nanoparticles for 2D and 3D Metal Patterning. *Adv. Mater.* **2002**, *14*, 194−198.

(20) Maruo, S.; Fourkas, J. T. Recent Progress in Multiphoton Microfabrication. *Laser Photon. Rev.* **2008**, *2*, 100−111.

(21) Radha, B.; Kiruthika, S.; Kulkarni, G. U. Metal Anion-Alkyl Ammonium Complexes as Direct Write Precursors to Produce Nanopatterns of Metals, Nitrides, Oxides, Sulfides, And Alloys. *J. Am. Chem. Soc.* **2011**, *133*, 12706−12713.

(22) Richmonds, C.; Sankaran, R. M. Plasma-Liquid Electrochemistry: Rapid Synthesis of Colloidal Metal Nanoparticles by Microplasma Reduction of Aqueous Cations. *Appl. Phys. Lett.* **2008**, *93*, 131501−03.

(23) Lee, S. W.; Kumpfer, J. K.; Lin, P. A.; Li, G.; Gao, X. P. A.; Rowan, S. J.; Sankaran, R. M. In Situ Formation of Metal Nanoparticle Composites Via "Soft" Plasma Electrochemical Reduction of Metallosupramolecular Polymer Films. *Macromolecules* **2012**, *45*, 8201−8210.

(24) Zhang, W.; Zhang, A.; Guan, Y.; Zhang, Y.; Zhu, X. X. Silver-Loading in Uncrosslinked Hydrogen-Bonded Lbl Films: Structure Change and Improved Stability. *J. Mater. Chem.* **2011**, *21*, 548−555.

(25) Lahav, M.; Narovlyansky, M.; Winkleman, A.; Perez-Castillejos, R.; Weiss, E. A.; Whitesides, G. A. Patterning of Poly(acrylic acid) by Ionic Exchange Reactions in Microfluidic Channels. *Adv. Mater.* **2006**, *18*, 3174−3178.

(26) Winkleman, A.; Perez-Castillejos, R.; Lahav, M.; Narovlyansky, M.; Rodriguez, L. N. J.; Whitesides, G. M. Patterning Micron-Sized Features in a Cross-Linked Poly(Acrylic Acid) Film ay a Wet Etching Process. *Soft Matter* **2007**, *3*, 108−116.

(27) Lebedev, E. A.; Süptitz, P.; Willert, I. Transport of Silver Under the Influence of an Electric Field in Glassy As_2Se_3. *Phys. Status Solidi (a)* **2006**, *28*, 461−466.

(28) Nge, T. T.; Nogi, M.; Suganuma, K. Electrical Functionality of Inkjet-Printed Silver Nanoparticle Conductive Tracks on Nanostructured Paper Compared with Those on Plastic Substrates. *J. Mater. Chem. C* **2013**, *1*, 5235−5243.

(29) Scardaci, V.; Coull, R.; Lyons, P. E.; Rickard, D.; Coleman, J. N. Spray Deposition of Highly Transparent, Low-Resistance Networks of Silver Nanowires over Large Areas. *Small* **2011**, *7*, 2621−2628.

(30) Lili, L.; Dan, Y.; Le, W.; Wei, W. Electroless Silver Plating on The Pet Fabrics Modified with 3-Mercaptopropyltriethoxysilane. *J. Appl. Polym. Sci.* **2011**, *124*, 1912−1918.

Supporting Information

Fabrication of electrically-conductive metal patterns at the surface of polymer films by microplasma-based direct writing

Souvik Ghosh,[†] *Rui Yang,*[‡] *Michelle Kaumeyer,*[‡] *Christian A. Zorman,*[‡] *Stuart J. Rowan,*[§] *Philip X.-L. Feng,*[‡] *and R. Mohan Sankaran*[†]*

[†]Department of Chemical Engineering, Case Western Reserve University, Cleveland, OH, U.S.A.

[‡]Department of Electrical Engineering and Computer Science, Case Western Reserve University, Cleveland, OH, U.S.A.

[§]Department of Macromolecular Sciences and Engineering, Case Western Reserve University, Cleveland, OH, U.S.A.

Keywords: microplasma, direct write, printed electronics, flexible electronics, sheet resistance

1. Preparation of Ag/PAA films

0.255 g of PAA (M_w = 1.26 million, Sigma-Aldrich) was mixed with 25 ml DI water and 75 ml ethanol. The mixture was left to stir overnight at room temperature in a covered conical flask. Complete dissolution of the polymer resulted in a colorless solution. A desired amount of $AgNO_3$ (Alfa-Aesar) was dissolved in a mixture of 5 ml DI water and 15 ml ethanol. The mixture was stirred at room temperature in a dark room until all the salt has dissolved. This mixture was added drop-wise to the conical flask while stirring vigorously. After all the $AgNO_3$ was added, the clear solution turned colorless to milky white. The solution produced a white precipitate which was assumed to be a Ag/PAA complex. Excess ethanol (~150 ml) was added to ensure complete precipitation. The precipitate was recovered by centrifuging (model RC-5C, Sorvall Instruments) at 10,000 rpm for 15 min, then decanting off the clear supernatant liquid. The precipitate was re-dissolved in a solution of water and ethylene glycol (6:1 by volume). The weight of this solution was varied depending on the concentration of the precursor. For precipitates containing a high Ag^+:[COOH] (*i.e.*, 0.64), a 20 wt% solution was used. The solution was homogenized with a Cole Parmer LabGen 7 homogenizer to break up the precipitate and obtain a low viscosity for film preparation. After homogenizing, the precipitate was vacuum dried for ~1 min until all the bubbles were removed.

Films were cast by a doctor's blade technique. The doctor's blade consists of a vertical blade that can be adjusted to a specific height from the base using two micrometers. We used a commercially available doctor's blade coater from MTI Corporation (Model EQ-Se-KTQ-150). Si (100) wafers were fixed on top of a glass plate with a small piece of double-sided tape. The homogenized precipitate was put on top of the wafers with a spatula. After setting the doctor's blade at a desired height, the blade was rapidly swept across the wafer. The film thicknesses could be varied by controlling the height of the doctor's blade. This produced a homogeneously covered thin film over the Si substrate (Figure S1). The casted films were dried overnight in the dark and then vacuum dried for another 3-4 h before microplasma exposure.

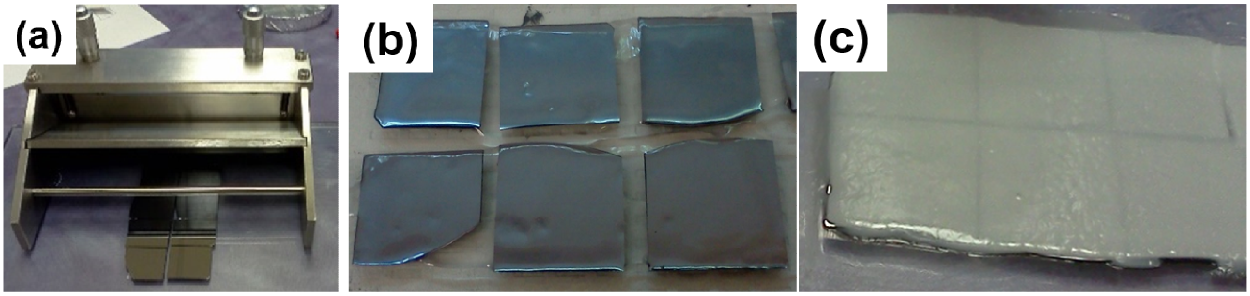

Figure S1. (a) Optical image of a 150 mm wide doctor's blade that was used to prepare thin films of Ag/PAA, (b) as-cast undried films with Ag^+:[COOH] = 0.32:1, (c) as-cast undried films with Ag^+:[COOH] = 0.64:1.

2. Microplasma exposure

A DC scanning microplasma was used to pattern the Ag/PAA thin films. Details of the experimental setup have been previously reported.[1,2,3] Briefly, the microplasma jet was formed in a flow of Ar gas using a stainless steel capillary tube (Restek Inc.). The Ar gas flow rate was controlled at 60 sccm with a digital mass flow controller. A negative high voltage supply (Keithley, Inc. Model 246) connected in series with a 500 kΩ ballast resistor was used to operate the microplasma with the capillary tube as the cathode and the Si substrate as the anode (ground). The substrate was placed on a computer-controlled x-y stage with a maximum scanning distance of 12 x 12 cm. The microplasma was ignited at ~1 kV by bringing the capillary tube close to the surface of the casted Ag/PAA film. The voltage was then reduced to obtain a desired discharge current. All experiments in this study were carried out at a constant voltage of 700 V and a discharge current of ~1–1.1 mA. The microplasma was scanned across the film over a distance of 5 mm at a constant scan rate (discussed below).

In our experiments, we found from visual inspection that the patterned line width depended on many of the process parameters including discharge current, electrode gap (distance between the end of the capillary tube and the film surface), gas flow rate, Ag^+:[COOH] ratio, film thickness, and scan rate. Of these, the scan rate was found to be one of the most important parameters. In order to more carefully assess the relationship between line width and scan rate and ultimately determine the minimum line width that could be obtained from this process, we carried out a systematic set of experiments. After patterning, the line widths were measured by imaging the film surface with an optical microscope and analyzing the digital images with ImageJ. Line widths were measured along the same line, on multiple lines drawn on the same substrate, and on different lines on different substrates.

Representative optical images of lines produced by the scanning microplasma process on 20 μm thick films containing Ag^+:[COOH] = 0.32 at various scan rates are shown in Figure S3. The images indicate that narrower lines are produced as the scan rate is increased. In addition, the edge acuity, i.e. the variation in line width along the line, is more significant at the lower scan rates studied here (100 and 125 μm/sec). These measurements were repeated on approximately 10 lines for each scan rate. Figure S3 shows the average line width as a function of the scan rate. The error bars indicate the variance in the line width at each scan rate. From these results, we can more clearly conclude that increasing the scan rate leads to a decrease in the patterned line width with a minimum line width of ~300 μm at scan rates > 250 μm/sec. The variation in line width exhibits a minimum of ±15 μm at a scan rate of 250 μm/sec.

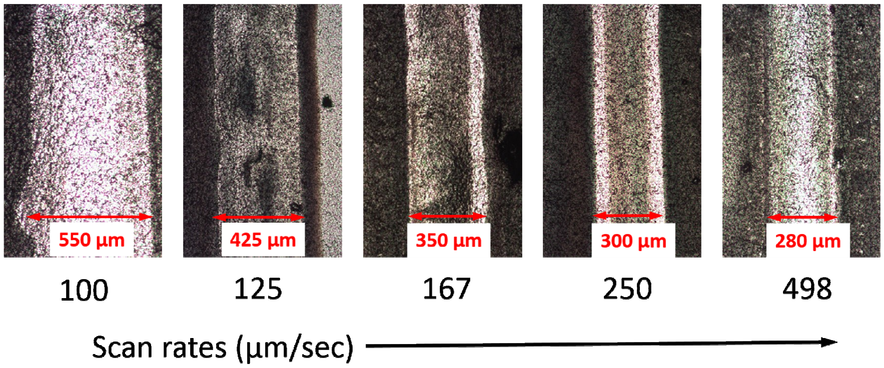

Figure S2. Representative optical images of lines patterned on 20 µm thick films containing Ag^+:[COOH] = 0.32 by the scanning microplasma process at various scan rates.

We interpret these results as the following. Based on our proposed electrophoretic model for Ag^+, the electric field created by the microplasma in the film should have an axial component (normal to the film and along the axis of the microplasma jet), but also a radial component (parallel to the film surface and perpendicular to the microplasma jet) since the microplasma acts as a point source at the top of the film. We suggest that at low scan rates (<250 µm/sec), the Ag^+ has more time to migrate to the surface (or more Ag^+ is able to migrate to the surface) and the radial component allows the Ag^+ to migrate laterally or add to the growing Ag film at the surface, resulting in wider lines. At higher scan rates (>250 µm/sec), there is less time for the Ag^+ to migrate to the surface (or less Ag^+ migrates), and the Ag is primarily formed along the axial direction, *i.e.*, directly below the microplasma which is approximately 300 µm in diameter. At very high scan rates (500 µm/sec), the variation in line width may be caused by fluctuations and instabilities in the microplasma. The Ag/PAA film is initially insulating and the microplasma-induced electrophoresis of Ag^+ to the surface of the film and reduction to metallic Ag increases the local conductivity, thereby stabilizing the microplasma. This effect may be reduced when the microplasma is scanned too fast and there is insufficient time for the Ag^+ to migrate, react, and grow. Based on this analysis, 250 µm/sec was selected as the scan rate for all experiments in this study.

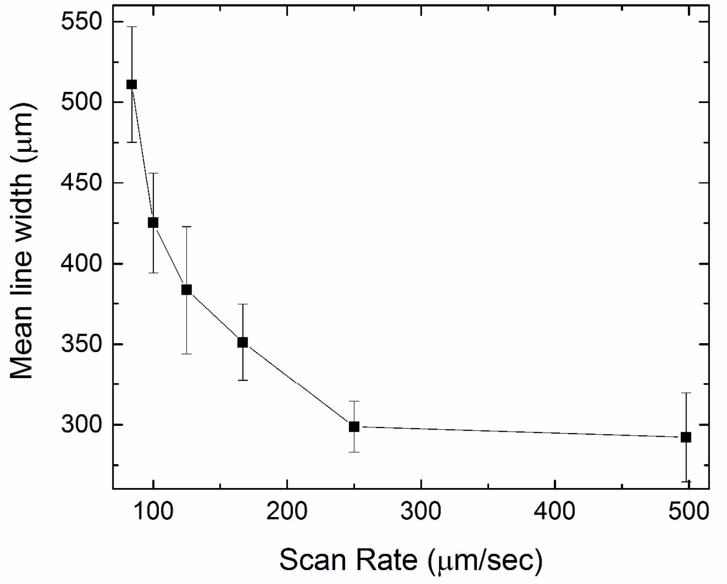

Figure S3. Average width of lines patterned on 20 µm thick films containing Ag^+:[COOH] = 0.32 by scanning microplasma process as a function of scan rate.

3. Characterization of microplasma-reduced lines

In order to perform electrical measurements on the microplasma-reduced lines, the films were peeled off from the Si substrate and placed on top of a polymer sheet of poly(ethylene) terephthalate (PET). Contact pads with Ag paste were made at the ends of the lines. Two-point probe measurements were carried out with a Keithley 4200 SCS. Figure S4 shows a schematic of the experimental setup. The samples were placed inside an EMI shielding chamber during current-voltage (I-V) measurements. More than 30 measurements were taken for a given sample to obtain an average I-V curve.

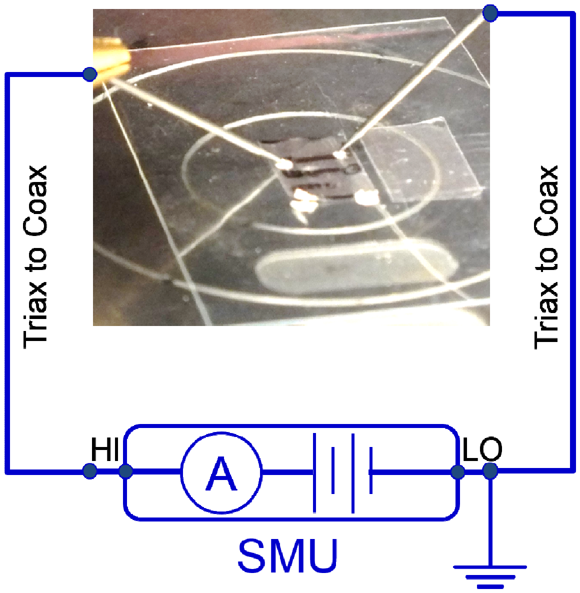

Figure S4. Schematic of two-point probe measurement of microplasma-reduced lines by a semiconductor measurement unit (SMU) that was connected to micromanipulator probes.

Figure S5 shows the average resistances obtained by two-point probe I-V measurements of the backside of microplasma-reduced Ag/PAA films containing different ratios of Ag^+:[COOH]. Bulk resistivities of the microplasma-reduced lines were calculated assuming that the Ag-rich surface layer was 5 μm thick. Figure S6 shows a summary of the estimated bulk resistivities for lines patterned in Ag/PAA films containing different Ag^+:[COOH] ratios. All films had a total thickness of >20 μm to minimize the resistance based on our proposed Ag^+ diffusion/reaction model.

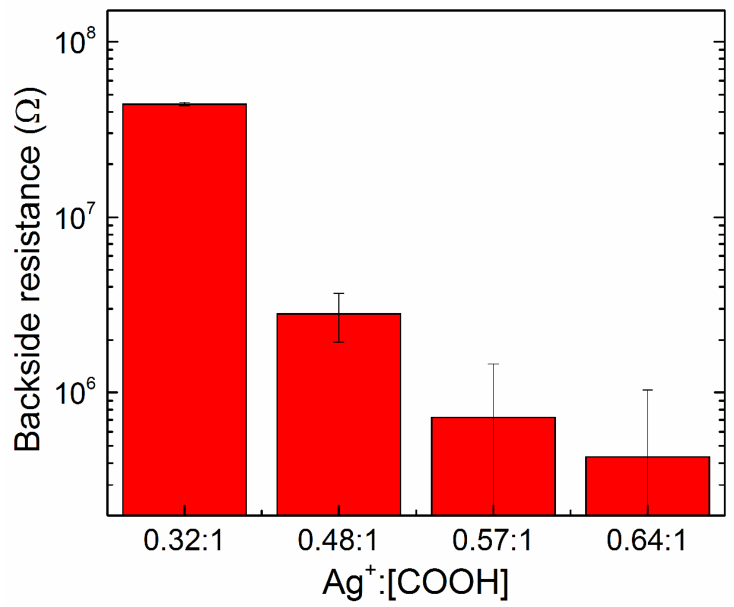

Figure S5. Average resistances obtained by two-point probe measurements on the back side of microplasma-reduced Ag/PAA films containing different Ag$^+$:[COOH] ratios.

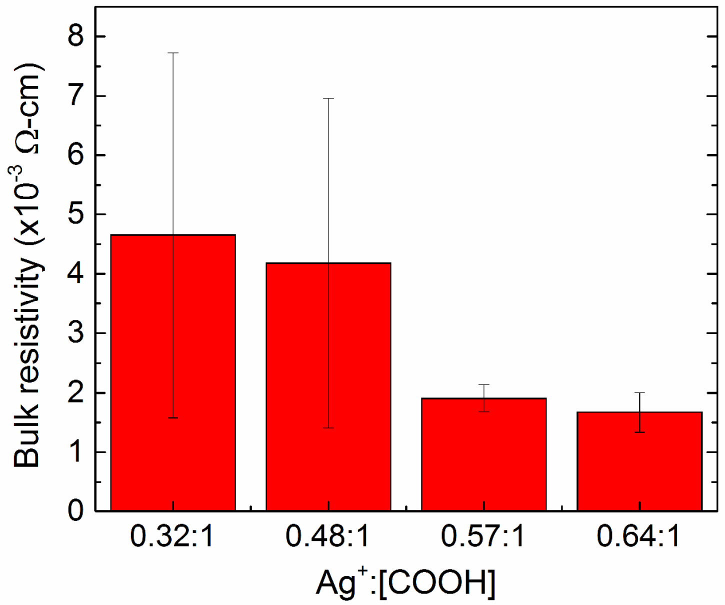

Figure S6: Bulk resistivities of microplasma-reduced lines of Ag/PAA films containing different Ag$^+$:[COOH] ratios. A surface layer of Ag of 5 μm was assumed in all cases. The total thickness of the films was >20 μm in all cases.

SEM and EDX characterization were performed with an FEI NOVA scanning electron microscope with a field emission gun and on-board EDS spectroscopy system. The SEM characterization was done at 5 kV and a working distance of 5 mm. The EDX analysis was done at varying acceleration voltages ranging between 10-15 kV, depending on the count-rate and minimization of the dead time. Figure S5 shows complementary false color EDX maps of the C and O content within a FIB-etched microplasma-reduced line. The images show that the C and O concentration increase from the film surface into the reduced feature.

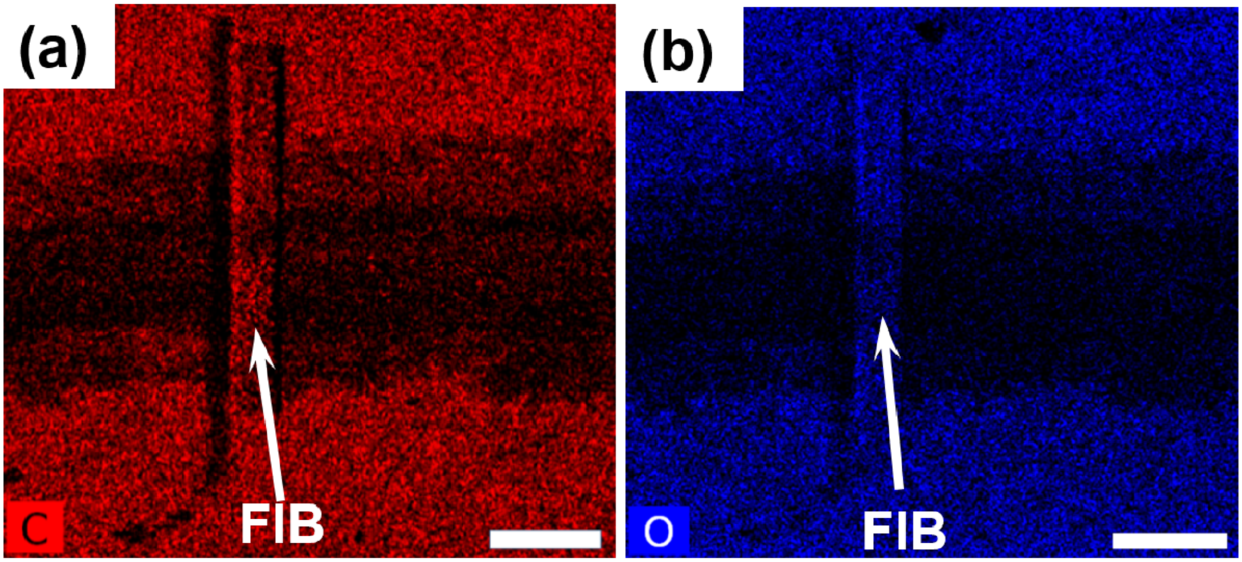

Figure S7. EDX false color maps of (a) carbon (b) oxygen content along a microplasma-reduced line of Ag/PAA. All scale bars are 100 μm. The FIB etched feature shows that the carbon and oxygen concentration are lower at the film surface than within the film bulk as a result of Ag precipitation and concomitant decrease in the PAA concentration.

Figure S8 shows a SEM image at the edge of a microplasma reduced line which has been cut to expose the cross-sectional area. An Ag-rich layer consisting of agglomerated Ag particles is observed near the surface of the film.

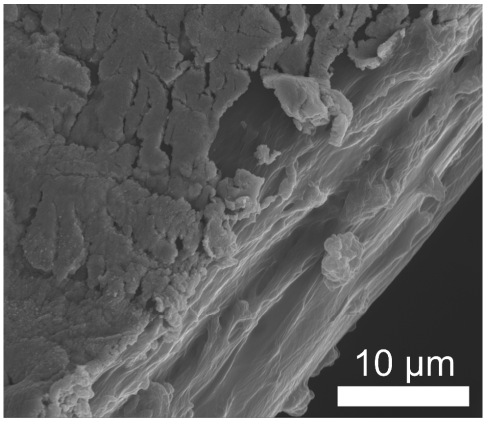

Figure S8. SEM image of a sectioned microplasma-reduced line showing a Ag-rich layer at the surface of the film.

Film thicknesses were obtained with a K-6 KLA Tencor stylus profilometer. On each Si substrate, half of the film was cut from the center and peeled off to use the bare substrate as a baseline. The profiler was scanned across the edge of the film over a distance of 5 mm that was equally distributed between the film and the substrate in order to measure the step-height. The step-height was measured at 5 regions of each substrate and averaged to get the average film thickness.

X-ray diffraction (XRD) was performed with a Scintag X-1 XRD. Scans were carried out in normal mode from 20^{o}-80^{o} in 0.05^{o} steps. The peaks were analyzed by comparing to reference data for Ag (JCPDS file #87-0717).

4. Control experiments

$AgNO_3$ is known to be photosensitive. Argon plasmas produce UV light, in addition to the charged species (ions, electrons, etc.). In order to understand the possible effect of UV light on the reduction of Ag^+ in our films, the following control experiments were performed:

a. Grounded mesh to block electrons

A grounded stainless steel mesh was placed between the microplasma and the Ag/PAA film to remove electrons, but still allow UV light to transmit. A photograph of the setup is shown in Figure S9. After exposing the film to the microplasma with a grounded mesh, the film was characterized by XRD. As shown in Figure S10, no peaks corresponding to crystalline Ag were visible. This confirms that the UV from the microplasma is not responsible for the reduction of the Ag^+ ions in the Ag/PAA films.

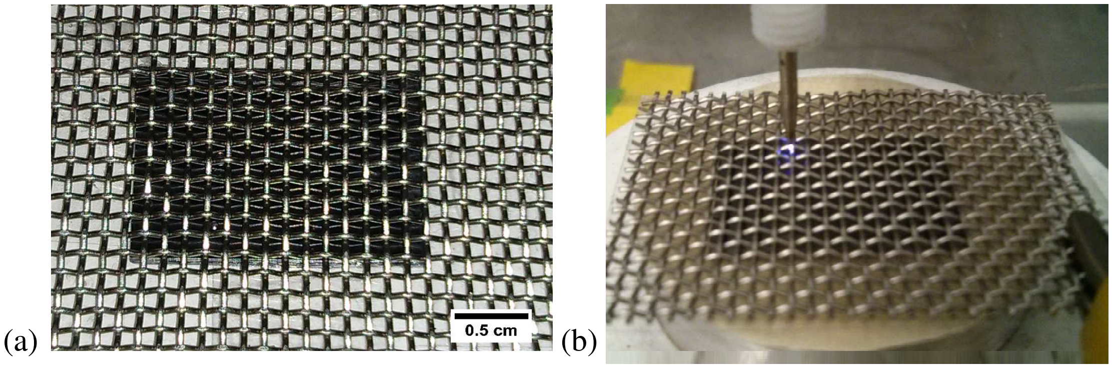

Figure S9. (a) Photograph of stainless steel wire mesh with 52% open area used to ground out electrons from the microplasma. (b) Photograph of microplasma scanning across a film containing Ag^+:[COOH] = 0.32 with the grounded mesh in place.

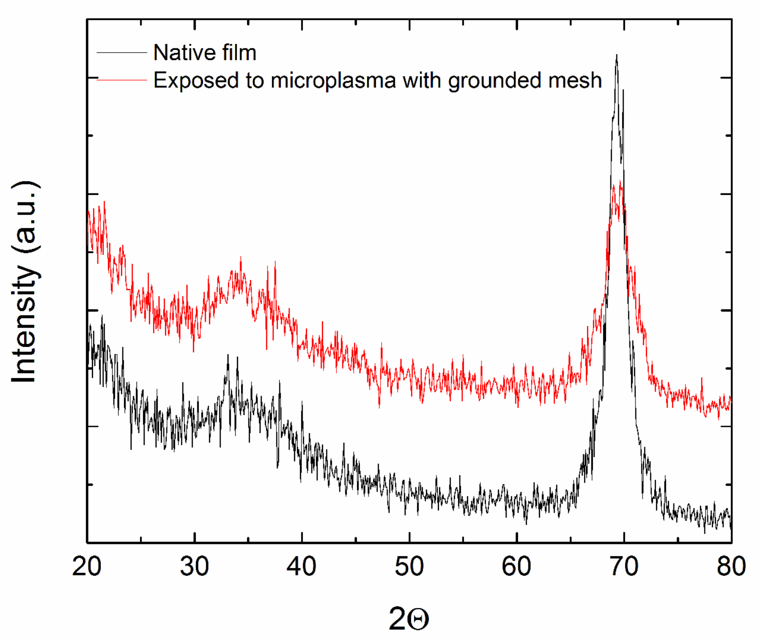

Figure S10. XRD characterization of a film containing Ag^+:[COOH] = 0.32 with a grounded mesh. A XRD scan of the unexposed film is also shown for comparison.

b. Characterization of UV light from microplasma

To further assess the UV light present in the microplasma, we collected and measured the optical emission with a light meter. To maximize the collection of light, the microplasma was formed in a closed chamber and the light was collected through a 3 mm diameter hole at the anode side of the microplasma jet with a 0.5 cm^2 detector (Coherent, Inc. Model OP-2 VIS) connected to a power meter (Coherent Inc, Fieldmate) (Figure S11a). The intensity at 405 nm was estimated to be 15 μW at a discharge voltage of 1.5 kV and discharge current of 3 mA (Figure S11b).

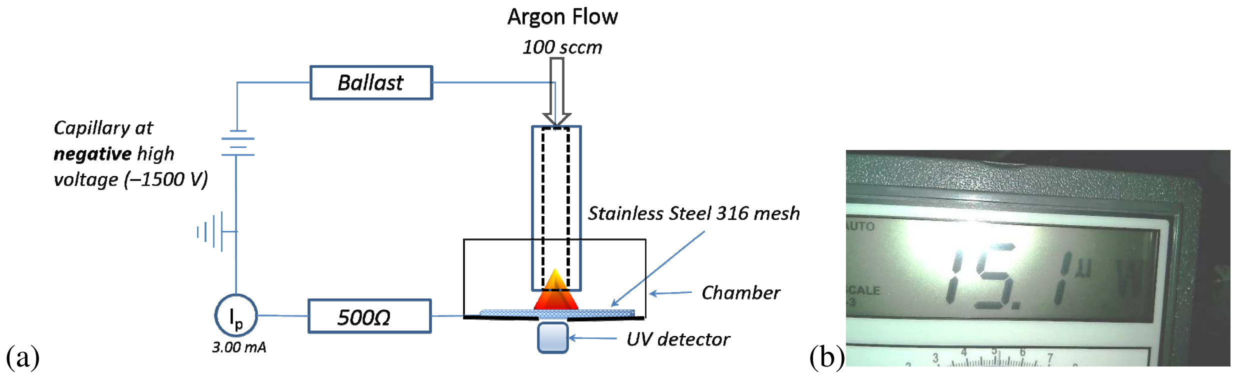

Figure S11. (a) Schematic of experimental setup for characterization of UV light emission from the microplasma. (b) Intensity of the 405 nm line in μW measured by a light meter which had an effective detector area of 0.5 cm^2.

c. *Exposure of Ag/PAA films to 405 nm diode laser*

To further assess whether the Ag^+ in the films could be reduced by UV light, we exposed the films to a solid-state laser. Our setup consisted of a 405 nm diode laser source mounted on a microscope with a 10x and 50x objective. The incident power at the film surface was measured to be 1.5 mW – we note that this is much higher than that measured in the microplasma. Films containing Ag^+:[COOH] = 0.32 were scanned by a motorized stage at rates similar to the microplasma process to create 5 mm x 1 μm lines. We initially characterized the lines by electrical measurements. I-V characteristics in Figure S12 show resistances of ~10^{12} Ω and indicate that no appreciable increase in conductivity was obtained after laser exposure. We also carried out XRD characterization on these films and found no evidence of crystalline material (Figure S13).

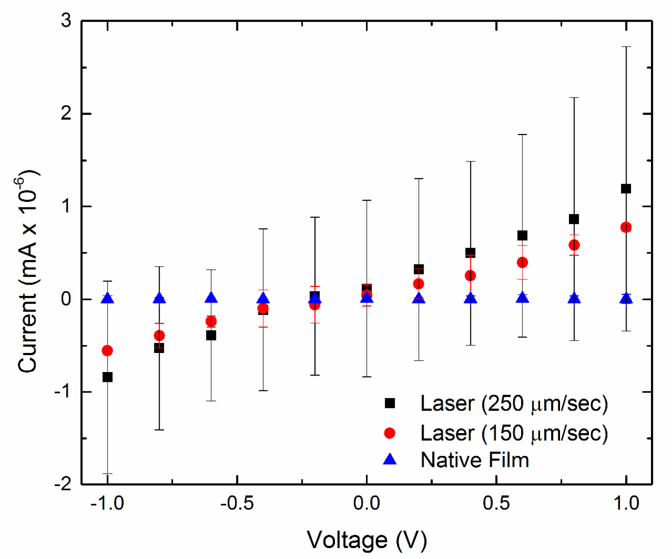

Figure S12. I-V characteristics of 5 mm x 1 μm lines fabricated in Ag$^+$:[COOH] = 0.32 films by scanning a 405 nm diode laser at an incident power of 1.5 mW. The I-V characteristic of the native film is shown for comparison.

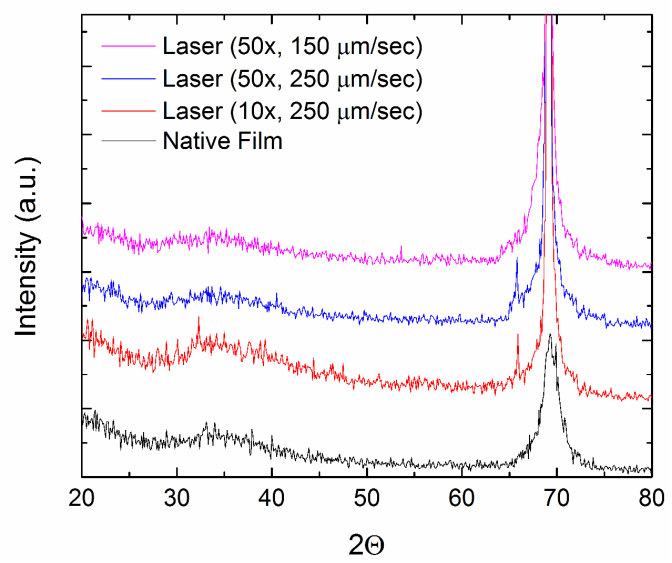

Figure S13. XRD characterization of Ag$^+$:[COOH] = 0.32 films exposed to a 405 nm diode laser at an incident power of 1.5 mW at different scan rates and through different microscope objectives.

d. Exposure of Ag/PAA films to UV lamp

As an alternative source of UV light, we exposed the Ag/PAA films to a UV lamp (Honle UV America, Inc.). We could vary the intensity and wavelength of the UV lamp; here, we used a bandpass filter to select the 320-500 nm wavelength range which overlaps with the laser experiments and the light measured from the microplasma. Films containing Ag^+:[COOH] = 0.32 were exposed at intensities of 10, 34, and 100 mW/cm^2 for 5 min. Figure S14 shows optical images of the samples after UV exposure. Although some color changes could be observed at higher powers indicating Ag^+ reduction, the films did not show any visual evidence of metallic Ag as in the case of microplasma reduction. This was confirmed by XRD which did not show any peaks corresponding to crystalline Ag (Figure S15).

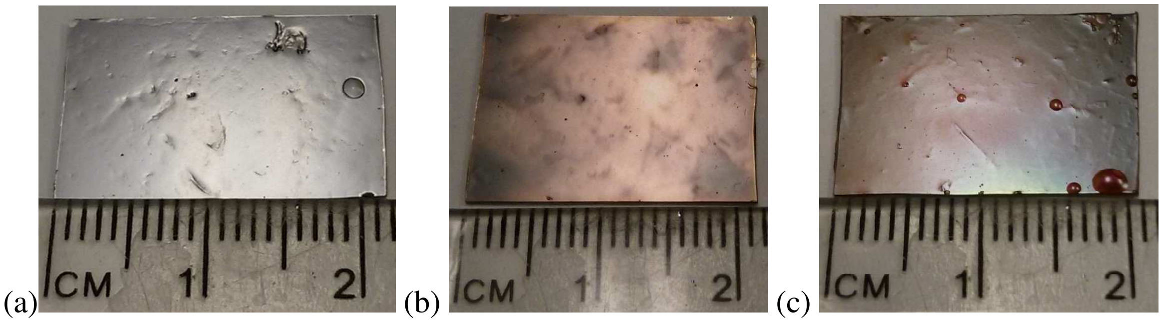

Figure S14. Optical images of Ag^+:[COOH] = 0.32 films exposed to a UV lamp between 320 and 500 nm at intensities of (a) 10 mW/cm^2, (b) 34 mW/cm^2, and (c) 100 mW/cm^2 for 5 min.

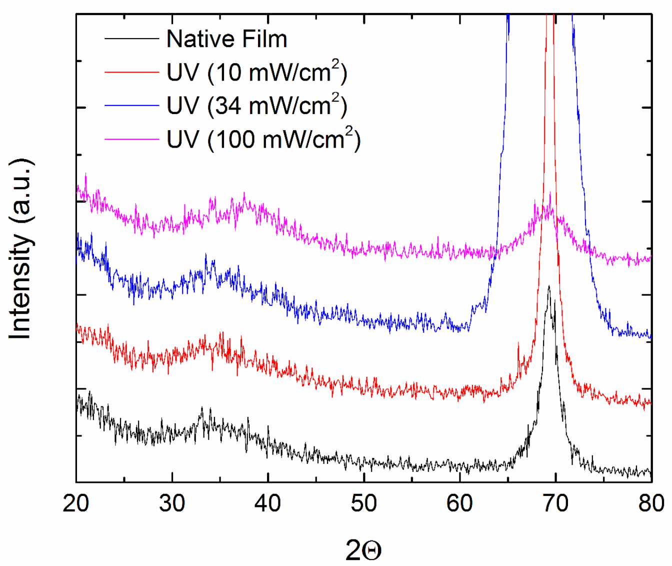

Figure S15. XRD characterization of Ag$^+$:[COOH] = 0.32 films exposed to a UV lamp between 320 and 500 nm at different intensities for 5 min. The XRD spectrum of the native film is shown for comparison.

References

---

(1) Richmonds, C.; Sankaran, R. M. Plasma-Liquid Electrochemistry: Rapid Synthesis of Colloidal Metal Nanoparticles by Microplasma Reduction of Aqueous Cations *Appl. Phys. Lett.* **2008**, *93*, 131501

(2) S. W. Lee, J. K. Kumpfer, P. A. Lin, G. Li, X. P. A. Gao, S. J. Rowan, R. M. Sankaran, In Situ Formation of Metal Nanoparticle Composites via "Soft" Plasma Electrochemical Reduction of Metallosupramolecular Polymer Films *Macromolecules*, **2012**, *45*, 8201.

(3) S. W. Lee, R. M. Sankaran, Direct Writing via Electron-Driven Reactions *Mater. Today*. **2013**, *16*(4), 117-122.